Journal of Animal & Plant Sciences, 35(2): 2025, Page: 612-624
ISSN (print): 1018-7081; ISSN (online): 2309-8694
https://doi.org/10.36899/JAPS.2025.2.0052

EFFECT OF VASCULAR ENDOTHELIAL GROWTH FACTOR SIRNA-LOADED NANOPARTICLES WITH DOXORUBICIN IN INHIBITING THE GROWTH OF BREAST CANCER IN XENOGRAFT MOUSE MODEL

X. H. Li, S. Y. Sun, X. C. Yue, S. Zhang, L.Y. Qian, J. Tang, F. Q. Jiang, J. F. Lu, Y. F. Cao, S. W. Meng, and T. J. Yao*

Four Wards of Thyroid and Breast, Department of Oncology Surgery, The First Affiliated Hospital of Bengbu Medical College, Bengbu, 233000, Anhui, China.
*Corresponding author's Email: yaotingjingah@126.com

ABSTRACT

As an antineoplastic antibiotic, doxorubicin (DOX) effectively inhibits RNA and DNA synthesis. However, its application is limited by side effects and drug resistance. This study established a xenograft mouse model of breast cancer (BC) to investigate the therapeutic efficacy of a gene/drug nano-delivery system combining vascular endothelial growth factor (VEGF) silencing with DOX for treating BC. Poly (lactic acid) (PLA) was utilized as the carrier material to prepare nanoparticles (NPs) loaded with VEGF interference RNA (siRNA) and the chemotherapeutic drug DOX (PLA/DOX-NPs and PLA/DOX-siVEGF-NPs). The characterization and drug release of NPs were analyzed. NPs' cytotoxicity was determined by CCK-8 assay with HUVEC and MCF-7 cells. The BC xenograft (BCX) model was established by injecting MCF-7 cells into the mammary fat pads of nude mice. The differences in tumor weight and tumor inhibition rate were analyzed after treatment with DOX alone, PLA/DOX-NPs, and PLA/DOX-siVEGF-NPs. Immunohistochemical staining was employed to examine Ki-67 positive expression rate in the BCXs. Western blot was used to detect Ki-67 and VEGF protein expression levels in transplanted tumor tissues. Additionally, a suspension of BCX cells was injected subcutaneously into healthy nude mice to assess tumor growth after secondary engraftment. Both PLA/DOX-NPs and PLA/DOX-siVEGF-NPs demonstrated sustained release of DOX in buffer media at varying pH values, with no visible difference in inhibiting human umbilical vein endothelial cells (HUVECs) proliferation. After establishment of the BCX mouse model, compared to DOX group, the PLA/DOX-NPs group and PLA/DOX-siVEGF-NPs group exhibited a significant reduction in relative tumor volume and Ki-67 index, along with an increased tumor inhibition rate. Furthermore, after secondary tumor formation, both tumor volume and size were markedly reduced (P<0.05). There were statistically significant differences in various parameters between the PLA/DOX-NPs group and the PLA/DOX-siVEGF-NPs group (P<0.05). The prepared PLA/DOX-siVEGF-NPs demonstrated low toxicity to normal cells and strongly inhibited the proliferation of MCF-7 BC cells *in vitro*. Moreover, PLA/DOX-siVEGF-NPs effectively inhibited the growth of BCXs in nude mice and suppressed Ki-67 positive expression. This treatment also reduced the malignant differentiation of the tumors and inhibited tumor recurrence.

Key words: xenograft mouse model, doxorubicin; nanoparticles; breast cancer; vascular endothelial growth factor.

Published first online April 03, 2025 Published final April 28, 2025

INTRODUCTION

Breast cancer (BC) poses a significant threat to women's health, and chemotherapy remains the mainstay of treatment for BC (Guo and Sun 2022). However, it falls short of achieving a definitive cure, and its long-term efficacy is not satisfactory. As a result, repeated and high-dose combination therapies are prone to induce drug resistance, while causing severe adverse reactions in multiple organs and tissues of patients (Iwamoto *et al.,* 2020). Doxorubicin (DOX) is an antineoplastic drug applied to treat various cancers (Jamialahmadi *et al.,* 2021; Wang and Jiang 2022). However, DOX has notable side effects, particularly cardiotoxicity, which significantly limits its clinical application (Hamanishi *et al.,* 2021).

In recent years, nano-drug has experienced rapid development in disease prevention and treatment. The United States has already approved the market release of liposomal formulations of Amphotericin B, DOX, and Daunorubicin, while paclitaxel nanoformulations have also been applied in clinical disease treatment (Barenholz 2012). Compared to traditional chemotherapy drugs, nano-drug can enhance the solubility of poorly soluble drugs and prolong their half-life in the body. Nanoparticles (NPs) with diameters ranging from 20 to 200 nm can passively target at tumor tissues (Kopeckova *et al.,* 2019; Karaosmanoglu *et al.,* 2021). In contrast to

small molecule formulations, small interfering RNA (siRNA) exhibits characteristics such as prolonged molecular action, high specificity, and gene silencing, making it a crucial tool in cancer therapy (Mainini and Eccles 2020). Vascular endothelial growth factor (VEGF) siRNA can suppress tumor angiogenesis by inhibiting VEGF expression and has become an important approach for inhibiting tumor growth (Jin *et al.,* 2022). However, the hydrophilic nature of siRNA makes it challenging to penetrate cell membranes with negative charges, resulting in a short half-life in the bloodstream and easy degradation by nucleases, thereby limiting its clinical application (Jin *et al.,* 2021). Polylactic acid (PLA), as a biodegradable polymer material, possesses good biocompatibility and biodegradability, making it widely used in drug delivery applications (Solechan *et al.,* 2023; Charbe *et al.,* 2020). Encapsulating siRNA within a PLA carrier effectively addresses issues such as its short half-life and susceptibility to degradation, enhancing the stability and delivery efficiency of siRNA (Repp *et al.,* 2021). This strategy overcomes the limitations of siRNA in clinical applications and provides a more effective approach for gene therapy.

In summary, there is currently a lack of an effective approach that integrates the advantages of NP-based drugs and siRNA for the coordinated delivery of chemotherapy agents and anti-angiogenic genes in BC treatment. This study aims to address this research gap. To enable the co-delivery of DOX and VEGF siRNA, PLA-based NPs, namely PLA/DOX-siVEGF-NPs, were prepared in this research. After characterization and analysis, the toxic effects of these NPs on human umbilical vein endothelial cells (HUVECs) and their *in vitro* cytotoxicity against MCF-7 were evaluated. Furthermore, an MCF-7 BCX model was fabricated to validate the *in vivo* antitumor efficacy of PLA/DOX-siVEGF-NPs. The main objective was to investigate the synergistic effects of anti-angiogenesis genes combined with chemotherapy drugs in BC tumor treatment, and to provide research insights for exploring novel approaches for BC therapy.

MATERIALS AND METHODS

Preparation of PLA-carried NPs: 250 mg of lactic acid (LA) (Shanghai Haohong Biotechnology Co., Ltd., China) was dissolved in 30 mL of dimethylformamide. Then, 233 mg of 1-(3-dimethylaminopropyl)-3-ethylcarbodiimide hydrochloride and 139 mg of N-hydroxysuccinimide were added separately, stirred at 50 °C for 45 minutes. 500 mg of PLL (Hangzhou Gutuo Biotechnology Co., Ltd., China) was allowed a dissolution in 30 mL of deionized water and slowly mixed with LA solution with stirring. Reaction lasted at 50 °C for 24 hours. The resulting solution was dialyzed in dialysis bag in deionized water for 48 hours. After filtration through a membrane filter (0.45 μm pore size) (Millipore, USA), the solution was freeze-dried to obtain PLA powder. 20 mg of PLA powder was dissolved in deionized water, and 1 mL of 10 mg/mL DOX·HCl solution (Wuhan Qianyan Chemical Technology Co., Ltd., China) and 0.5 μL of triethylamine were added. After stirring for 5 minutes using a magnetic stirrer (Shanghai Meijingpu Instrument Manufacturing Co., Ltd., China), the mixture was dialyzed to remove triethylamine and free DOX. After filtration again, PLA/DOX-NPs were obtained. The VEGF siRNA sequence was synthesized. The sense strand was 5'-GGAGUACCCUGAUGAGAUCUU-3', and the antisense strand was 5'-GAUCUCAUCAGGGUACUCCUU-3'. 100 nmol of siRNA was mixed with PLA/DOX-NPs solution in a nitrogen-to-phosphorus ratio of 6:1 (Aydin *et al*., 2022), which was stirred for 15 minutes. Following a standing still, PLA/DOX-siVEGF-NPs solution was obtained. The integrity of siRNA was assessed using gel electrophoresis.

Characterization and quality evaluation: The process involved using ultrapure water for dilution of PLA/DOX-NPs and PLA/DOX-siVEGF-NPs. NPs' morphology was observed using scanning electron microscope (SEM, GYR Nock Testing Technology Co., Ltd., Germany), and the average particle size and surface zeta potential were measured using dynamic light scattering instrument (DLS, Model ASXRD, Anhui Guoke Instrument Technology Co., Ltd., China). To determine drug concentration, the NPs were disrupted using ethanol and then diluted. A microplate reader (Shandong Hengmei Technology Co., Ltd., China) measured the fluorescence intensity with excitation and emission at 590 and 480 nm, respectively. For drug release studies, an appropriate amount of NP suspension was subjected to a 30-min centrifugation at 12,000 rpm at 4°C. Fluorescence intensity in supernatant was measured, and free drug concentration was also determined.

To simulate the physiological and intracellular environments, this research selected phosphate buffer solutions (PBS) with pH of 7.4 and 5.3 as release media. PBS at pH 7.4 was used to simulate the physiological environment, with a composition of 137 mM NaCl, 2.7 mM KCl, 10 mM Na_2HPO_4, and 1.8 mM KH_2PO_4. PBS at pH 5.3 was used to mimic the intracellular environment, with a composition similar to that of PBS at pH 7.4, but the pH adjustment was achieved by altering the ratio of phosphate monobasic and phosphate dibasic salts. 3 mL of PLA/DOX-NPs and PLA/DOX-siVEGF-NPs were placed in separate MWCO 3500 Da dialysis bags (Shanghai Moli Biotechnology Co., Ltd., China). The bags were then immersed in wide-mouth bottles containing 100 mL of the release media, maintained at 37°C with constant shaking at 100

rpm. At 0.25, 0.5, 1, 3, 6, 12, 24, and 48 h, 1 mL of release medium outside the bag was discarded and replaced with 1 mL fresh release medium at same temperature. DOX concentration in release medium was determined. Cumulative drug release rate was calculated and then a time-cumulative release rate curve was plotted.

Determination of *in vitro* cytotoxicity: MCF-7 (Cell Resource Center, China) and HUVEC (Cell Resource Center, China) were seeded at 1×10^4 cells in a 96-well plate and performed with a 24-h incubation at 37°C with 5% CO_2 (Shanghai Rundu Biotechnology Co., Ltd., China). Medium was then replaced with fresh ones containing DOX, PLA/DOX-NPs, or PLA/DOX-siVEGF-NPs at 0.05, 0.5, 5, 25, 50, 100, 200, and 500 μg/mL. The plate was incubated for an additional 48 hours in them. Afterward, 100 μL of CCK-8 reagent (Sigma-Aldrich, USA) was placed, and the plate was further incubated for 1.5 hours. Optical density was measured at 450 nm, and cell viability was calculated.

Detection of transplanted tumor volume and tumor inhibition rate: 2×10^6 logarithmic growth phase MCF-7 were inoculated into the right subcutaneous region of 30 female BALB/c-Nude mice (5 weeks old, 18 g body weight; Beijing Vital River Laboratory Animal Technology Co., Ltd., China). The mice were housed at (25.5±1.5) °C with a humidity of (55±10) %. All procedures were approved by the Ethical Committee of hospital and responsible authorities of research organization(s) following all guidelines, regulations, legal, and ethical standards as required.

Once the tumors reached approximately 1 cm^3 in size, 24 BCX mice (transplanted successfully) were randomly divided into four groups (each with 6 mice): BC group (BCX model), DOX group, PLA/DOX-NPs group and PLA/DOX-siVEGF-NPs group. BC group received an equivalent volume of physiological saline, the DOX group received 25 mg/kg of DOX, and the PLA/DOX-NPs group and PLA/DOX-siVEGF-NPs group were respectively given a suspension of NPs containing 25 mg/kg of DOX. The mice's survival status and changes in body weight were monitored, and a time-body weight curve was plotted. The BCX tumor size was measured regularly, and on day 22, mice were euthanized by cervical dislocation. Tumor tissues were harvested and weighed. Tumor inhibition rate was calculated.

Weight changes in nude mice with transplanted tumor: The transplanted tumor tissue was placed in a sterile Petri dish, and the cell suspension was prepared by using ophthalmic scissors and adjusted to 2×10^{10} cells/L. The mice outer thigh skin was disinfected. Then, each group of mice was inoculated with 50 μL of the respective cell suspension. The mice were kept under routine conditions, and the tumor growth was observed daily. The growth curve was plotted to monitor tumor development. After 14 days, the mice were euthanized to harvest tumors, which were weighed to evaluate tumor growth.

Immunohistochemical detection: Transplanted tumor tissues were fixed with 4% paraformaldehyde solution for 6 h and then embedded in paraffin after gradient alcohol dehydration. With phosphate buffer as negative control, Ki-67 level in Ki-67 transplanted tumor tissues was detected by immunohistochemical staining kit (Sigma-Aldrich, USA). Under a microscope, the stained sections were observed, and the nuclei of Ki-67 positively stained cells appeared brownish-yellow or brown. Five random fields were chosen for counting the number of positively stained cells, and the Ki-67 index was calculated. The Ki-67 index was a measure of the percentage of cells with positive staining for the Ki-67 protein, which was an indicator of cellular proliferation. It was calculated by dividing the number of Ki-67 positively stained cells by total cell number counted in the selected fields and then multiplying by 100 to get the percentage. The Ki-67 index provided valuable information about the proliferative activity of the tumor cells.

Western blotting: The tumor tissue (0.2 g) was rinsed with PBS and lysed with protein lysis buffer at a ratio of 3:1 (v/v) for 15 minutes. Supernatant was collected after centrifugation to obtain the protein sample, whose concentration was determined utilizing bicinchoninic acid methodology or another protein quantification method. The proteins were separated by sodium dodecyl sulphate-polyacrylamide gel electrophoresis. After gel cutting, proteins were transferred onto a polyvinylidene fluoride membrane (Sigma, USA) to be blocked with 5% non-fat milk in Tris buffered saline Tween (TBST) buffer at 25°C for 1 hour. After membrane rinsing with TBST buffer, primary antibodies (Ki-67 at 1:2,000 dilution, VEGF at 1:1,000 dilution, and GAPDH at 1:2,000 dilution, all from Sigma, USA) were added and incubated overnight at 4°C. Following another wash with TBST buffer, membrane was incubated with horseradish peroxidase-conjugated IgG secondary antibodies (Sigma, USA) at 25°C for 2 hours. After final washing with TBST buffer, chemiluminescent detection was implemented utilizing an electrochemiluminescence (ECL) chemiluminescence detection kit (Amersham Pharmacia, Sweden). The protein bands were visualized and imaged employing Invitrogen iBright gel imaging system (Thermo Fisher, USA). *ImageJ* was employed for densitometry analysis to quantify relative grayscale values of the target proteins.

Statistical analysis: *SPSS 22.0* was employed. Quantitative data were presented as mean±standard deviation. One-way analysis of variance (ANOVA)

compared data among multiple groups. For post-hoc analysis of pairwise comparisons between groups, the Least Significant Difference (LSD) methodology was applied. $P<0.05$ was utilized to determine statistical significance of a difference.

RESULTS

Characterization of PLA-carried NPs: Both prepared PLA/DOX-NPs and PLA/DOX-siVEGF-NPs had a circular shape. The average particle size values of both NPs were measured. From Figure 1A, it was evident that the average particle size values of PLA/DOX-NPs and PLA/DOX-siVEGF-NPs were (141.9±10.3) nm and (163.5±12.9) nm, respectively. Figure 1B exhibited that the average surface zeta potential values of them were (-10.7±0.8) mV and (-14.3±1.3) mV, respectively. From Figure 1C, EE values of PLA/DOX-NPs and PLA/DOX-siVEGF-NPs were (89.8±5.9) % and (85.1±4.6) %, respectively. As given in Figure 1D, the drug-loading capacity values of PLA/DOX-NPs and PLA/DOX-siVEGF-NPs were (15.2±1.4) % and (10.7±1.0) %, respectively.

In vitro, pH = 5.3 was selected to simulate the intracellular tumor microenvironment, while pH = 7.4 was utilized to simulate the blood circulation environment, to investigate the drug release characteristics of the prepared NPs. As demonstrated in Figure 2A, in PBS with pH = 5.3, the DOX drug release rate values of PLA/DOX-NPs and PLA/DOX-siVEGF-NPs gradually increased, with (23.5±1.4) % and (19.9±1.2) % at 48 hours, respectively. Similarly, when pH = 7.4 (Figure 2B), the DOX drug release rate values of both PLA/DOX-NPs and PLA/DOX-siVEGF-NPs also gradually increased, which reached (40.9±2.3) % and (36.5±2.1) % at 48 hours, respectively.

Cytotoxicity characteristics of co-loaded PLA NPs *in vitro*: As illustrated in Figure 3, with increasing drug and NP concentrations, proliferation activity of HUVECs gradually decreased. However, no significant differences were observed in HUVEC proliferation activity among single-agent DOX, PLA/DOX-NPs, and PLA/DOX-siVEGF-NPs treatments.

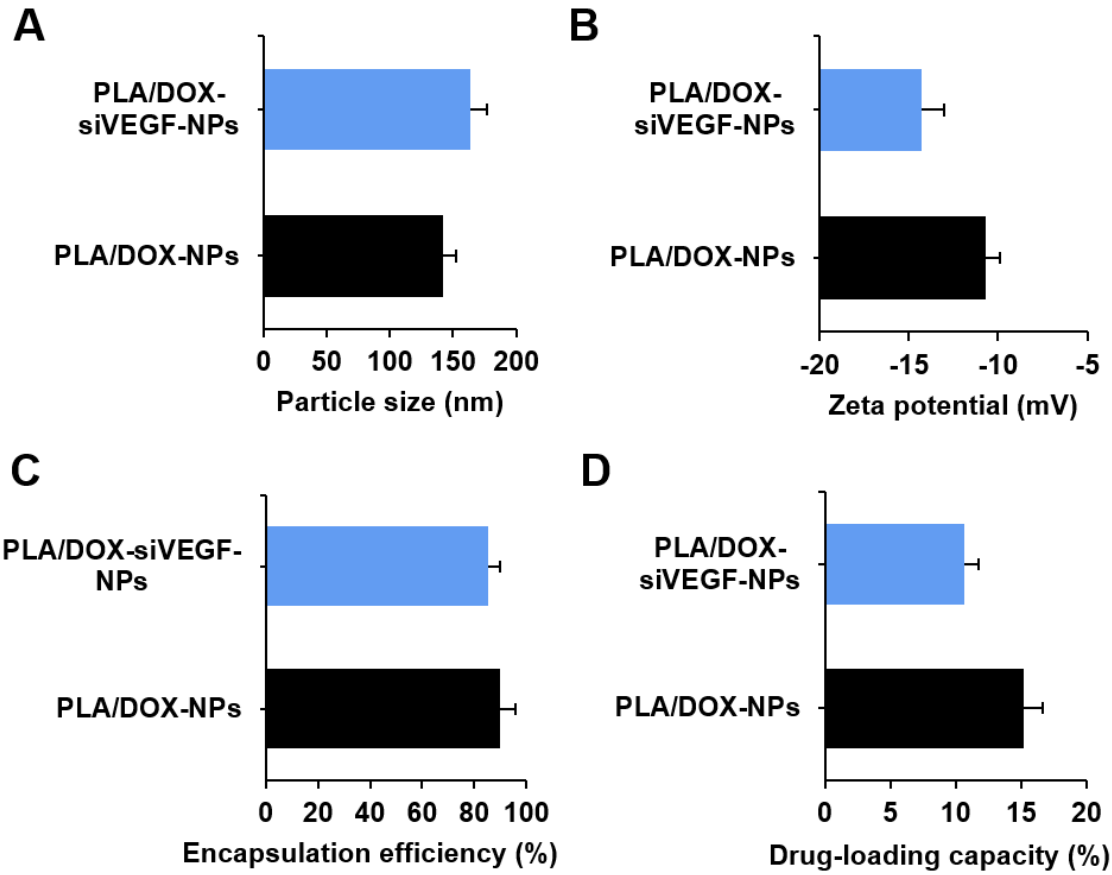

Fig. 1 Characterization of PLA NPs. A: average particle size; B: surface zeta potential; C: encapsulation efficiency; D: drug-loading capacity.

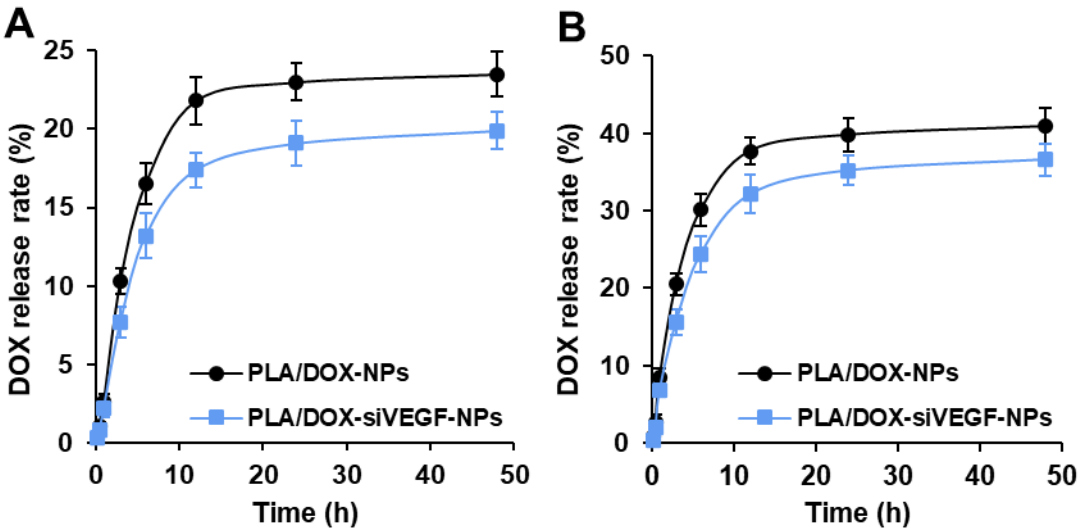

Fig. 2 The DOX cumulative release rate of PLA/DOX-NPs and PLA/DOX-siVEGF-NPs over time under simulated tumor intracellular microenvironment and simulated blood circulation environment. A: simulated tumor intracellular microenvironment, pH = 5.3; B: simulated blood circulation environment, pH = 7.4.

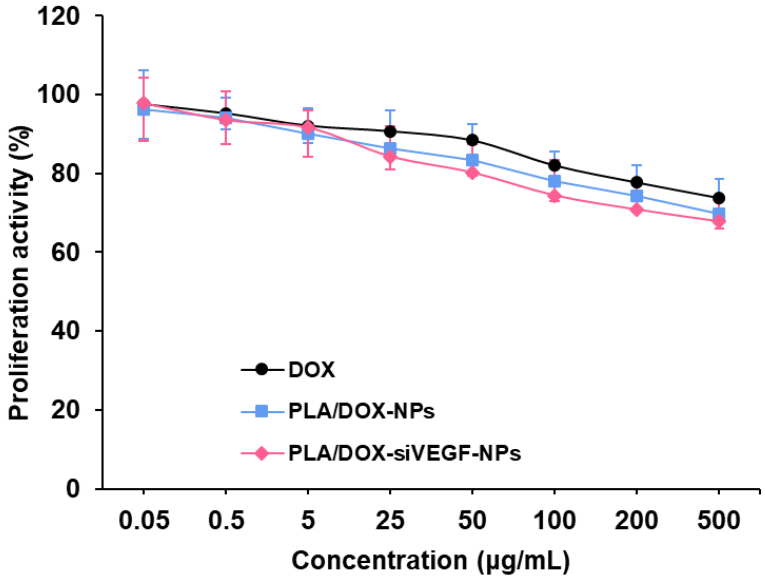

Fig. 3 The effect of DOX, PLA/DOX-NPs, and PLA/DOX-siVEGF-NPs on the proliferation ability of HUVECs. There were no statistically significant differences in the proliferation activity of HUVECs among the different groups.

The effects of single-agent DOX, PLA/DOX-NPs, and PLA/DOX-siVEGF-NPs on MCF-7 cell proliferation were first examined. As explicated in Figure 4, with increasing drug and NP concentrations, proliferation activity of MCF-7 cells gradually decreased. Based on DOX group, PLA/DOX-NPs and PLA/DOX-siVEGF-NPs group exhibited a more remarkable reduction in MCF-7 proliferation. Furthermore, in comparison to the PLA/DOX-NPs group, the PLA/DOX-siVEGF-NPs group exhibited a more pronounced decrease in MCF-7 proliferation.

Weight changes of nude mice transplanted with BC: The evaluation of body weight changes in BCX nude mice after treatment revealed the following findings (Figure 5). Firstly, based one BC group, the mice in DOX group, PLA/DOX-NPs group, and PLA/DOX-siVEGF-NPs group all presented an obvious reduction in body weight, showing great differences (P<0.05). Secondly, relative to DOX group, mice in PLA/DOX-NPs and PLA/DOX-siVEGF-NPs groups exhibited remarkable increase in body weight, exhibiting a considerable difference, too (P<0.05). Additionally,

mice in the PLA/DOX-siVEGF-NPs group suffered from a great increase in body weight, with a visible difference to those in PLA/DOX-NPs group (P<0.05).

Changes of transplanted tumor volume and tumor inhibition rate of BC in nude mice: Differences in BCX relative volume and tumor inhibition rate among various treatment groups were evaluated, as compared in Figure 6. Based on the BC group, mice in the DOX, PLA/DOX-NPs, and PLA/DOX-siVEGF-NPs groups exhibited a visible decrease in BCX volume but a considerable increase in tumor inhibition rate, possessing remarkable differences with P<0.05. Meanwhile, mice in the PLA/DOX-NPs and PLA/DOX-siVEGF-NPs groups showed sharp decrease in BCX volume and increase in tumor inhibition rate, having obvious differences with DOX group (P<0.05). Additionally, in contrast to PLA/DOX-NPs group, PLA/DOX-siVEGF-NPs group demonstrated a decreased BCX volume and but increase tumor inhibition rate (P<0.05).

Changes in BCX Ki-67 positive expression: Immunohistochemical staining was utilized to detect changes in Ki-67 positive expression rates (PERs) in BCX tumors of the different treatment groups. Results were summarized and compared in Figure 7 below. Ki-67-positive cells appeared as brown or tan staining, with the highest PER observed in the BC group. Mice in all groups except BC group exhibited a visible decrease in Ki-67 index, showing great differences (P<0.05). Furthermore, Ki-67 index in PLA/DOX-NPs and PLA/DOX-siVEGF-NPs groups was decreased versus DOX group (P<0.05). In addition, the PLA/DOX-siVEGF-NPs group demonstrated also a decreased Ki-67 index, demonstrating a great difference with PLA/DOX-NPs group (P<0.05).

VEGF and Ki-67 protein expression level of BC transplanted tumor in nude mice: From Figure 8, it is evident that relative to BC group, VEGF and Ki-67 protein expression levels in tumor tissues of mice treated with DOX, PLA/DOX-NPs, and PLA/DOX-siVEGF-NPs were drastically decreased (P<0.05). Relative to DOX group, VEGF and Ki-67 protein levels in tumor tissues of mice treated with PLA/DOX-NPs and PLA/DOX-siVEGF-NPs were also reduced (P<0.05). Additionally, PLA/DOX-siVEGF-NPs group showed decreased levels of VEGF and Ki-67 protein expression in tumor tissues versus DPLA/DOX-NPs group (P<0.05).

Secondary engraftment of BCX: The secondary engraftment of tumor cells in BCX nude mice was evaluated. Results were summarized as follows (Figure 9). Based on BC group, BCX mice in other groups exhibited decreased tumor volume and mass of secondary engraftment, and remarkable differences were observed (P<0.05). Based on DOX group, PLA/DOX-NPs and PLA/DOX-siVEGF-NPs groups presented greatly decreased volume and mass of secondary engraftment, also with great differences (P<0.05). Additionally, comparison between PLA/DOX-NPs and PLA/DOX-siVEGF-NPs were greatly different in volume and tumor mass of secondary engraftment (P<0.05).

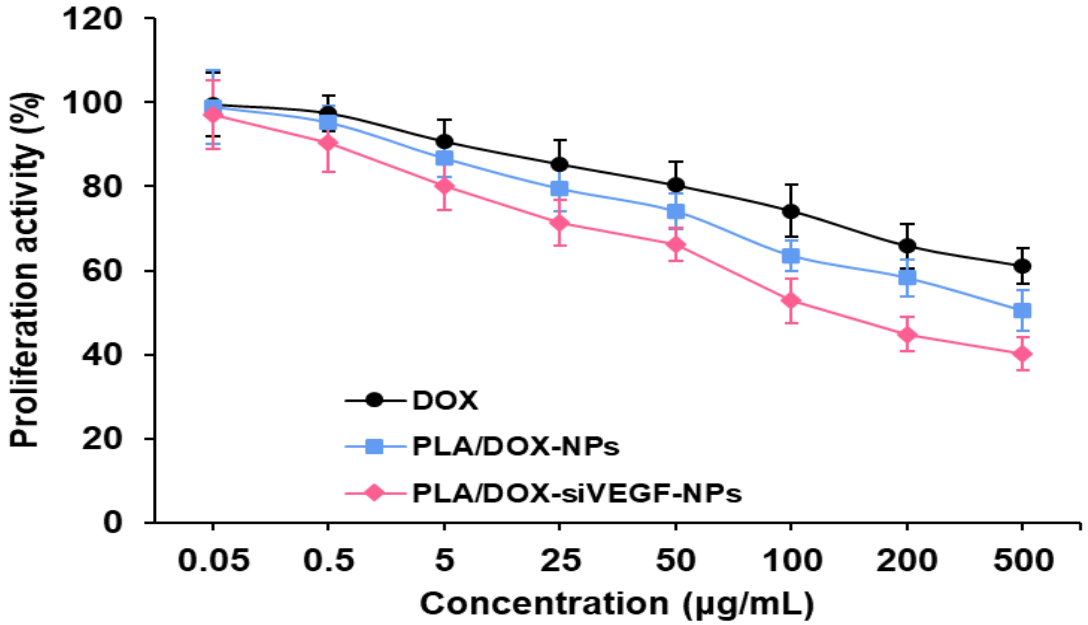

Fig. 4 The effect of DOX, PLA/DOX-NPs and PLA/DOX-siVEGF-NPs on proliferation of MCF-7. As the concentration of the drug and NPs increased, the proliferation activity of MCF-7 cells gradually decreased. The PLA/DOX-siVEGF-NPs group exhibited a more pronounced inhibitory effect on the proliferation of MCF-7 cells compared to the PLA/DOX-NPs group.

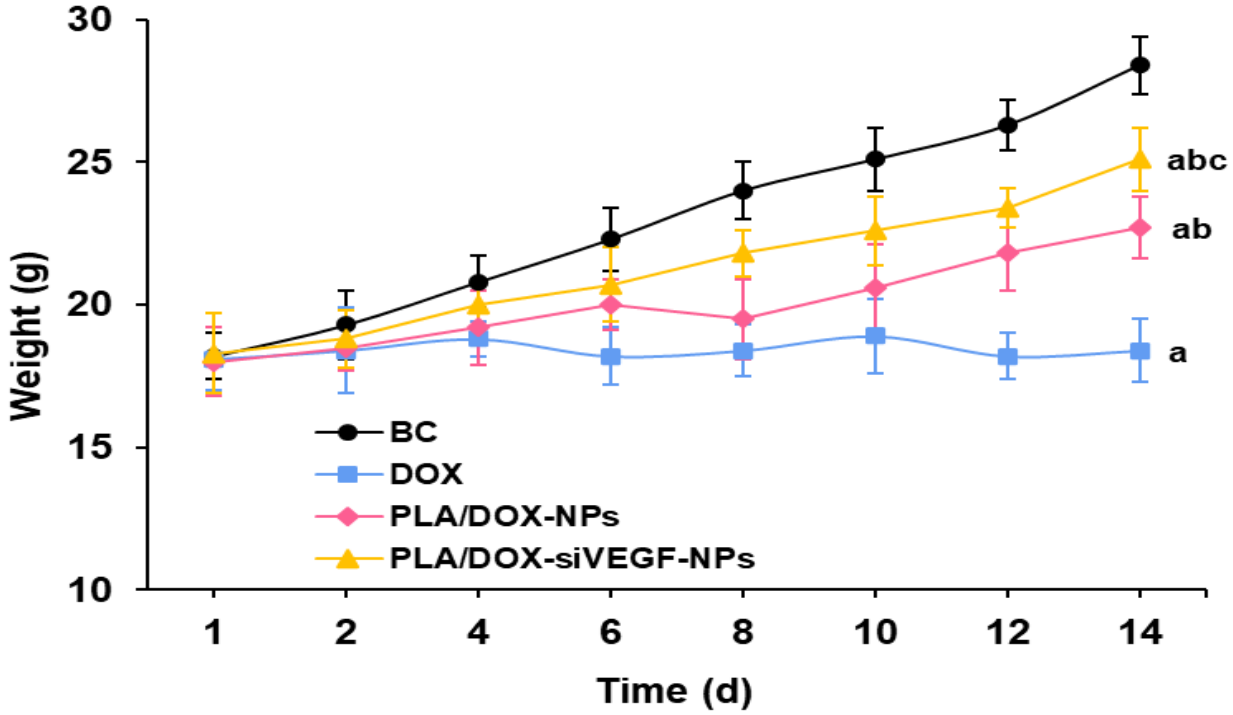

Fig. 5 Changes in body weight of mice in various groups. Note: [a]*P*<0.05 vs. BC group; [b]*P*<0.05 vs. DOX group; [c]*P*<0.05 vs. PLA/DOX-NPs group.

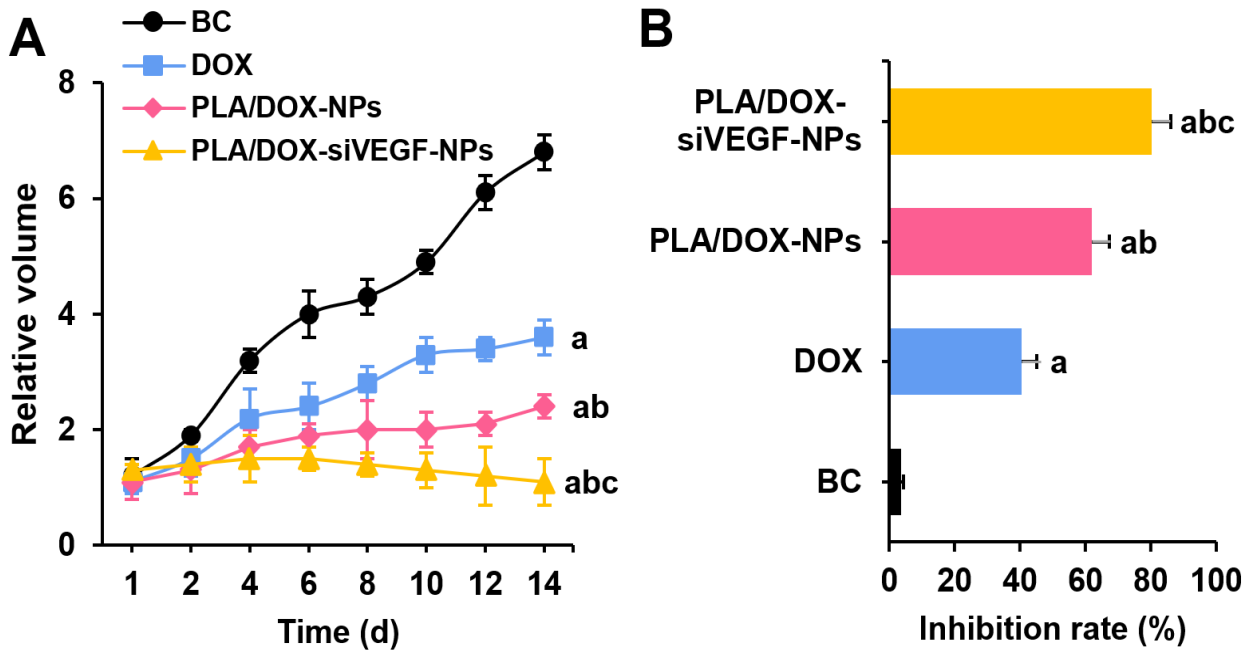

Fig. 6 Changes in BCX volume (A) and tumor inhibition rate (B) in mice from various groups. Note: [a]*P*<0.05 vs. BC group; [b]*P*<0.05 vs. DOX group; [c]*P*<0.05 vs. PLA/DOX-NPs group. The BCX volume in mice from the PLA/DOX-NPs and PLA/DOX-siVEGF-NPs groups significantly decreased compared to the DOX group, and the tumor inhibition rate was notably increased.

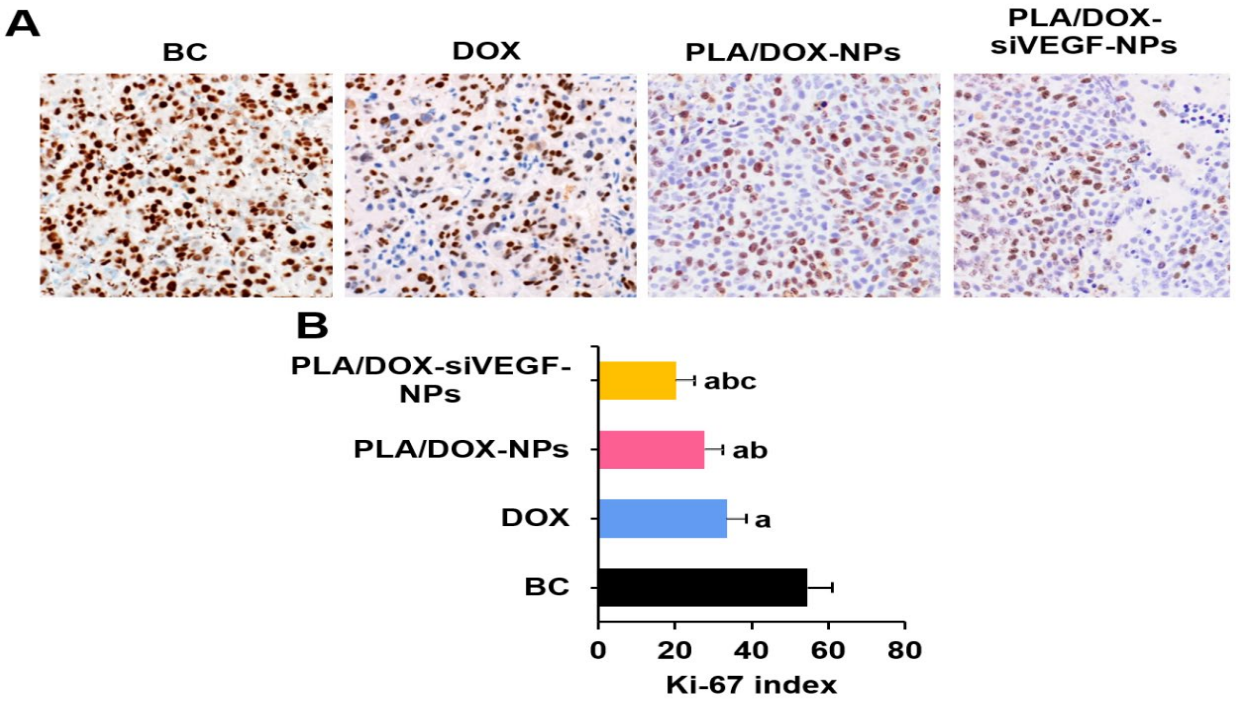

Fig. 7 Changes in positive staining results of BCX Ki-67. A: Immunohistochemical staining of Ki-67, ×200; B: Ki-67 index. Note: [a]*P*<0.05 vs. BC group; [b]*P*<0.05 vs. DOX group; [c]*P*<0.05 vs. PLA/DOX-NPs group. The Ki-67 index in the PLA/DOX-NPs and PLA/DOX-siVEGF-NPs groups decreased, with a more pronounced reduction observed in the PLA/DOX-siVEGF-NPs group.

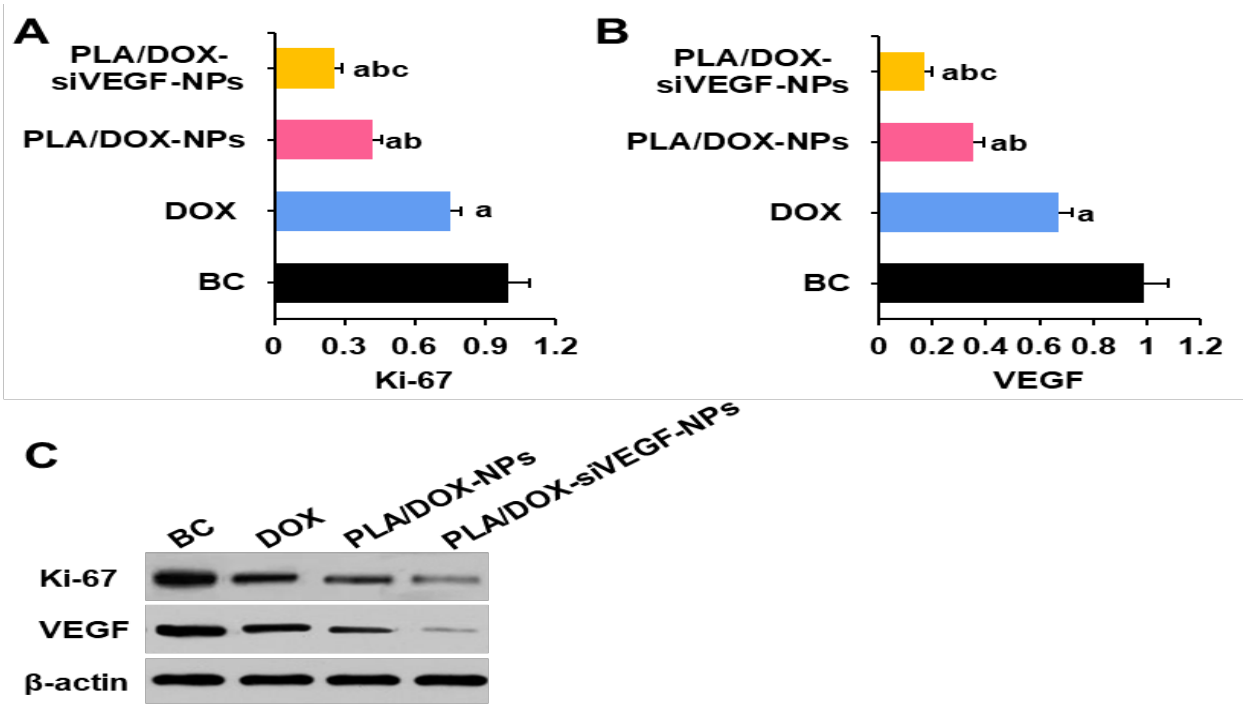

Fig. 8 Expression levels of VEGF and Ki-67 protein of transplanted tumor in nude mice in each group. A: Ki-67 protein level; B: VEGF protein level; C: Western blot. Note: [a]*P*<0.05 vs. BC group; [b]*P*<0.05 vs. DOX group; [c]*P*<0.05 vs. PLA/DOX-NPs group. The expression levels of VEGF and Ki-67 proteins in tumor tissues of mice from the PLA/DOX-NPs and PLA/DOX-siVEGF-NPs groups were reduced, with a more significant decrease observed in the PLA/DOX-siVEGF-NPs group.

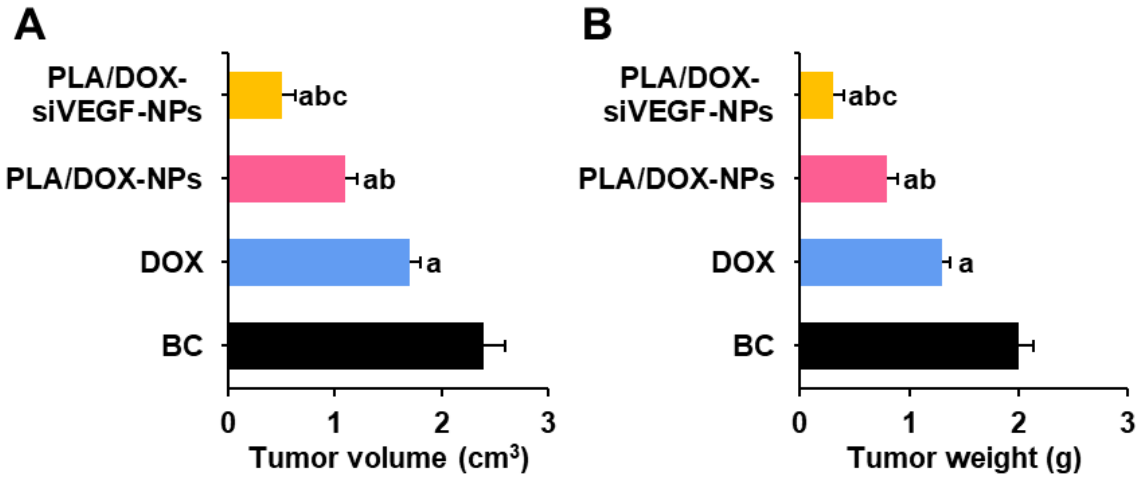

Fig. 9 The secondary engraftment of BCX in different groups. A: volume of secondary engraftment; B: mass of secondary engraftment. [a]*P*<0.05 vs. BC group; [b]*P*<0.05 vs. DOX group; [c]*P*<0.05 vs. PLA/DOX-NPs group. The volume and weight of the secondary transplanted tumors in the PLA/DOX-NPs and PLA/DOX-siVEGF-NPs groups were significantly reduced, with a more pronounced decrease observed in the PLA/DOX-siVEGF-NPs group.

DISCUSSION

This study explored the application of nanocarriers loaded with VEGF siRNA and DOX in BC treatment. Using PLA as the carrier material, NPs loaded with VEGF siRNA and chemotherapeutic drug DOX were prepared (PLA/DOX-NPs and PLA/DOX-siVEGF-NPs). The cytotoxicity of these NPs on human vascular endothelial cells and MCF-7 BC cells was evaluated using CCK-8 assays. In addition, the BC xenograft mouse model was established to further analyze the inhibitory effects of single-agent DOX, PLA/DOX-NPs, and PLA/DOX-siVEGF-NPs on tumor growth in nude mice, as well as their impact on Ki-67 and VEGF protein expressions. It was found that PLA/DOX-siVEGF-NPs not only exhibited low toxicity to normal cells but also effectively inhibited proliferation of MCF-7 cells. *In vivo*, these NPs demonstrated significant anti-tumor effects in the BC nude mouse model, reducing malignancy and suppressing tumor recurrence. This research highlighted the potential advantages and application value of PLA/DOX-siVEGF-NPs in BC therapy.

An appropriate particle size can influence the circulation time, tissue distribution, and cellular uptake efficiency of NPs *in vivo*. In this study, both PLA/DOX-NPs and PLA/DOX-siVEGF-NPs had particle sizes smaller than 200 nm, with PLA/DOX-siVEGF-NPs having a larger particle size. This could be attributed to the co-loading of DOX and VEGF small interfering RNA (siVEGF), where the additional siVEGF increases the NP volume. NPs with sizes in the range of 100-200 nm are favorable for passive targeting and accumulation in tumor sites via the enhanced permeability and retention effect, due to the high permeability of tumor tissues (Wu, 2021). Therefore, the particle sizes of both PLA/DOX-NPs and PLA/DOX-siVEGF-NPs are advantageous for their application in tumor therapy. The Zeta potential of NPs is a critical indicator of their stability, influenced by surface charge density (Mi *et al.,* 2021). In this study, both PLA/DOX-NPs and PLA/DOX-siVEGF-NPs exhibited negative Zeta potentials, with PLA/DOX-siVEGF-NPs showing a higher negative potential. This may be attributed to the addition of siVEGF, which increased the surface charge density of the NPs. NPs with negative Zeta potentials typically exhibit good biocompatibility in vivo, reducing non-specific adsorption to plasma proteins and cellular uptake, thereby prolonging their circulation time and enhancing drug accumulation at the target site (LoPresti *et al.,* 2022). Furthermore, the negative charge can enhance the stability of NPs in physiological solutions, preventing NP aggregation. Moreover, PLA/DOX-siVEGF-NPs showed a higher negative charge, indicating superior dispersibility, stability, and biocompatibility. Conventional chemotherapy drug DOX lacks tumor specificity and often leads to drug resistance, thereby reducing treatment efficacy (Ahmadpour *et al.,* 2021). NP drug delivery systems can enhance drug tumor targeting, efficiency, reduced toxicity, and controlled release (Ramasamy *et al.,* 2022). pH levels influence various biochemical reactions within the tumor microenvironment, affecting tumor cell growth and metastasis (Vitale *et al.,* 2019; Swietach 2019). In this study, both PLA/DOX-NPs and PLA/DOX-siVEGF-NPs systems demonstrated an increasing drug release trend under the acidic environment mimicking tumor cells,

which helps to enhance cytotoxicity against tumor cells under tumor microenvironment stimulation while reducing the side effects of DOX. Compared to acidic conditions, both NP systems exhibited slightly higher drug release rates in the pH 7.4 buffer solution simulating the blood environment, and both showed sustained drug release characteristics. This indicates that the two prepared NP systems possess drug sustained-release capabilities under different pH conditions, which is beneficial for prolonging the therapeutic effect of the drug. From a drug therapy perspective, the drug release characteristics of the NPs in the acidic tumor microenvironment allow DOX to specifically target tumor cells, improving its cytotoxic effects on tumor cells while minimizing unnecessary exposure to normal tissues, thus reducing systemic toxicity. This is crucial for enhancing the safety and efficacy of cancer treatment. In the blood environment, the NPs also maintained a certain level of sustained drug release, ensuring that the drug could be continuously and stably distributed and circulated in the body, maintaining an effective plasma concentration and prolonging the drug's therapeutic duration. This ability to achieve sustained drug release in different physiological environments strongly supports the application of NPs as drug carriers.

The results indicated that the proliferation activity of HUVECs decreased with increasing drug and NP concentrations, suggesting that these drugs and NP systems exhibit certain cytotoxicity against HUVECs. There were no significant differences in the effect on HUVEC proliferation between DOX, PLA/DOX-NPs, and PLA/DOX-siVEGF-NPs, implying that HUVECs may be less sensitive to these treatments. From a clinical perspective, this suggests that the damage to normal endothelial cells could be relatively consistent when using these drugs and NP systems. Additionally, we observed that as the drug and NP concentrations increased, the proliferation activity of MCF-7 BC cells gradually decreased. Compared to DOX alone, PLA/DOX-NPs and PLA/DOX-siVEGF-NPs exhibited a more pronounced inhibitory effect on MCF-7 cell proliferation. This could be due to the ability of NPs as drug carriers to enhance the stability and bioavailability of the drug. PLA NPs can protect DOX from enzymatic degradation and rapid clearance *in vivo*, allowing more drug to reach and act on tumor cells. Moreover, NPs may also more effectively accumulate in tumor tissues through active or passive targeting mechanisms, increasing drug concentration within tumor cells (Petersen *et al.,* 2024). The PLA/DOX-siVEGF-NPs group showed a more significant inhibition of MCF-7 cell proliferation compared to the PLA/DOX-NPs group, primarily attributed to the action of siVEGF.

VEGF can stimulate the proliferation, migration, and survival of endothelial cells, promoting the formation of tumor blood vessels that supply nutrients and oxygen to tumor cells, thereby supporting tumor growth and metastasis. PLA/DOX-siVEGF-NPs, by carrying VEGF siRNA, specifically silence the expression of the VEGF gene and reduce VEGF secretion. This leads to the inhibition of tumor angiogenesis and a reduction in the blood supply to the tumor, thus affecting the growth and survival of tumor cells. Previous studies have shown (Li *et al.,* 2021) that the expression level of VEGF is closely related to the malignancy of tumors, and reducing VEGF expression can suppress the invasion and metastatic ability of tumor cells, thus lowering the degree of malignant differentiation of the tumor. Meanwhile, DOX can embed into DNA molecules, inhibiting DNA and RNA synthesis, and thereby blocking tumor cell proliferation (Cao *et al.,* 2023). In PLA/DOX-siVEGF-NPs, DOX and VEGF siRNA work synergistically to enhance anti-tumor effects. On one hand, DOX directly acts on tumor cells, killing them; on the other hand, VEGF siRNA inhibits tumor angiogenesis, reducing the tumor's nutrient supply, making tumor cells more sensitive to DOX. This synergistic effect could be a key reason why PLA/DOX-siVEGF-NPs show superior performance in inhibiting tumor growth and reducing malignancy. The results of this study suggest that the PLA/DOX-siVEGF-NPs system has potential application value in inhibiting the proliferation of MCF-7 BC cells. This combination therapy strategy offers a new approach for BC treatment, potentially enhancing therapeutic effects while reducing toxic side effects on normal cells.

Ki-67 is a non-histone protein located within cell nuclei, and its quantity correlates positively with the malignancy of tumors (Luchini *et al.,* 2022). In BC patients, a higher rate of positive expression of Ki-67 in immunohistochemical staining indicates a higher malignancy of tumors, poorer prognosis for patients, and greater treatment challenges (Korpela *et al.,* 2021). The higher the proliferation activity of tumors, the higher the rate of Ki-67 positive expression, indicating faster tumor growth (Zhang *et al.,* 2021). Transplanting human or murine primary BC tissues or cells onto animals is a commonly used method for constructing BC models. This model offers advantages such as short cycles and low costs (Dekkers *et al.,* 2020). A xenograft model of BC was established. Immunohistochemical staining results showed a significant decrease in Ki-67 index in tumors from mice treated with DOX, PLA/DOX-NPs, and PLA/DOX-siVEGF-NPs. Particularly, the PLA/DOX-siVEGF-NPs group exhibited a significantly lower Ki-67 index compared to the PLA/DOX-NPs group and DOX alone group. This indicates that the NP can effectively inhibit tumor cell proliferation. Combining VEGF inhibition and the cytotoxic effects of DOX, we hypothesize that PLA/DOX-siVEGF-NPs exert a multi-target mechanism of action. They not only directly kill tumor cells but also inhibit tumor angiogenesis, thereby reducing the proliferative signals in tumor cells

and lowering the expression level of Ki-67. Concurrently loading VEGF interference RNA and DOX into NPs further enhanced the inhibitory effect on tumor cell proliferation. This enhanced effect may be attributed to additional inhibition of VEGF, potentially disrupting tumor blood supply and thereby enhancing therapeutic efficacy. These results further support the potential application of PLA/DOX-siVEGF-NPs as a promising strategy for BC treatment. VEGF is a crucial factor that promotes tumor lymphangiogenesis and facilitates tumor metastasis to regional lymph nodes and distant sites (Peng *et al.,* 2018; Harahap *et al.,* 2022). Elevated levels of VEGF have been confirmed in serum of patients with various malignancies such as BC (Maryam *et al.,* 2021). Overexpression of VEGF in tumor patients correlates with poor prognosis, serving as an independent prognostic factor for overall survival rates (Lin *et al.,* 2019). In BC, high expression of VEGF promotes the formation of new blood vessels within tumors, providing adequate blood supply to support rapid growth and dissemination, and is associated with tumor invasiveness and adverse prognosis (Banerjee *et al.,* 2023; Zhu *et al.,* 2020). Western blot results in the study indicated that compared to other groups, the PLA/DOX-siVEGF-NPs group exhibited significantly reduced levels of VEGF and Ki-67 protein expression in xenograft tumor tissues. This suggests that PLA/DOX-siVEGF-NPs effectively reduces VEGF expression and directly induces tumor cell death, providing a more effective therapeutic effect in inhibiting tumor proliferation and angiogenesis. The use of PLA/DOX-siVEGF-NPs enhances the efficacy of DOX while reducing VEGF and Ki-67 expression, improving modulation of the tumor microenvironment, inhibiting tumor proliferation, and angiogenesis. Thus, PLA/DOX-siVEGF-NPs represent a promising strategy for BC treatment. This research confirmed that PLA nanospheres co-loaded with the chemotherapeutic drug DOX and VEGF siRNA can effectively reduce the Ki-67 PER by silencing VEGF expression. This synergistic effect of VEGF silencing and chemotherapy with DOX can reduce the malignancy of BCX and ultimately inhibit the growth rate of BCX. In future work, we plan to demonstrate the therapeutic efficacy of PLA/DOX-siVEGF-NPs on different subtypes of BC and other types of tumors. Additionally, we aim to address the long-term toxicity and resistance issues of PLA/DOX-siVEGF-NPs to evaluate their safety and feasibility for extended treatment periods.

Conclusion: PLA/DOX/siVEGF-NPs exhibit a favorable drug release rate with minimal cytotoxicity to normal HUVECs, while demonstrating significant in vitro cytotoxicity against BC MCF-7 cells. The PLA/DOX/siVEGF-NPs NPs have minimal impact on the normal physiological state of nude mice, while enhancing tumor suppression, reducing BCX volume, and inhibiting the expression levels of Ki-67 and VEGF. The findings of this study provide a new perspective for the exploration of effective methods in BC treatment.

Funding: This work was supported by Humanities and Social Science Project of Bengbu Medical College (BYKY2019202skZD) and Key Project at the School Level of Bengbu Medical College (2021byzd096).

Statement: All authors have no conflicts of interest.

Authors' Contributions: Xuanhe Li, Siyu Sun and Tingjing Yao designed experiments; Xicheng Yue, Song Zhang, Liyu Qian, Jie Tang, Fangqian Jiang, Jianfei Lu, Yifan Cao, Shengwen Meng collected samples; Xuanhe Li, Siyu Sun and Tingjing Yao performed experiments; Xuanhe Li, Siyu Sun and Tingjing Yao analyzed data; Xuanhe Li, Siyu Sun and Tingjing Yao wrote the manuscript. All authors agreed to publish this article.

REFERENCES

Aydin, O., D. Kanarya, U. Yilmaz, and C.Ü. Tunç (2022). Determination of optimum ratio of cationic polymers and small interfering RNA with agarose gel retardation assay. Methods Mol. Biol., 2434, 117 – 128. https://doi.org/10.1007/978-1-0716-2010-6_7

Ahmadpour, S.T., V. Desquiret-Dumas, U. Yikilmaz, J. Dartier, I. Domingo, C. Wetterwald, C. Orre, N. Gueguen, L. Brisson, K. Mahéo and J.F. Dumas (2021). Doxorubicin-induced autophagolysosome formation is partly prevented by mitochondrial ROS elimination in DOX-resistant breast cancer cells. Int. J. Mol. Sci., 22(17), 9283. https://doi.org/10.3390/ijms22179283.

Barenholz, Y. (2012). Doxil®--the first FDA-approved nano-drug: lessons learned. J. Control Release, 160(2),117–134. https://doi.org/10.1016/j.jconrel.2012.03.020

Banerjee, K., T. Kerzel, T. Bekkhus, S. de Souza Ferreira, T. Wallmann, M. Wallerius, L.S. Landwehr, D.A. Agardy, N. Schauer, A. Malmerfeldt, J. Bergh, M. Bartish, J. Hartman, A. Östman, M.L. Squadrito and C. Rolny (2023). VEGF-C-expressing TAMs rewire the metastatic fate of breast cancer cells. Cell Rep., 42(12),113507. https://doi.org/10.1016/j.celrep.2023.113507.

Cao, Z., R. Liu, Y. Li, X. Luo, Z. Hua, X. Wang, Z. Xue, Z. Zhang, C. Lu, A. Lu and Y. Liu (2023). MTX-PEG-modified CG/DMMA polymeric micelles for targeted delivery of doxorubicin to induce synergistic autophagic death against triple-negative breast cancer. Breast Cancer Res., 25(1), 3.

https://doi.org/10.1186/s13058-022-01599-9

Charbe, N.B., N.D. Amnerkar, B. Ramesh, M.M. Tambuwala, H.A. Bakshi, A.A.A. Aljabali, S.C. Khadse, R. Satheeshkumar, S. Satija, M. Metha, D.K. Chellappan, G. Shrivastava, G. Gupta, P. Negi, K. Dua and F.C, Zacconi (2020). Small interfering RNA for cancer treatment: overcoming hurdles in delivery. Acta. Pharm. Sin. B., 10(11), 2075–2109. https://doi.org/10.1016/j.apsb.2020.10.005.

Dekkers, J.F., J.R. Whittle, F. Vaillant, H.R. Chen, C. Dawson, K. Liu, M.H. Geurts, M.J. Herold, H. Clevers, G.J. Lindeman and J.E. Visvader (2020). Modeling breast cancer using CRISPR-Cas9-mediated engineering of human breast organoids. J. Natl. Cancer Inst., 112(5),540–544. https://doi.org/10.1093/jnci/djz196.

Guo, Q.F. and J.Q. Sun (2022). Therapeutic effect of anti-miRNA mediated by RNA nanoparticles targeting CD133 on triple-negative breast cancer. Sci. Adv. Mater., 14(4), 803–809. https://doi.org/10.1166/sam.2022.4269.

Hamanishi, J., N. Takeshima, N. Katsumata, K. Ushijima, T. Kimura, S. Takeuchi, K. Matsumoto, K. Ito, M. Mandai, H. Nakai, N. Sakuragi, H. Watari, N. Takahashi, H. Kato, K. Hasegawa, K. Yonemori, M. Mizuno, K. Takehara, H. Niikura, T. Sawasaki, S. Nakao, T. Saito, T. Enomoto, S. Nagase, N. Suzuki, T. Matsumoto, E. Kondo, K. Sonoda, S. Aihara, Y. Aoki, A. Okamoto, H. Takano, H. Kobayashi, H. Kato, Y. Terai, A. Takazawa, Y. Takahashi, Y. Namba, D. Aoki, K. Fujiwara, T. Sugiyama and I. Konishi (2021). Nivolumab versus Gemcitabine or Pegylated Liposomal Doxorubicin for patients with platinum-resistant ovarian cancer: open-label, randomized trial in Japan (NINJA). J. Clin. Oncol., 39(33), 3671–3681. https://doi.org/10.1200/JCO.21.00334.

Harahap, W.A., T. Tofrizal and O. Oktahermoniza (2022). Relationship between the expression of BRAF V600E and Ki-67 with the recurrence of well-differentiated thyroid cancer. Asian Pac. J. Cancer Prev., 23(11),3617–3622. https://doi.org/10.31557/APJCP.2022.23.11.3617.

Iwamoto, T., Y. Kajiwara, Y. Zhu and S. Iha (2020). Biomarkers of neoadjuvant/adjuvant chemotherapy for breast cancer. Chin Clin Oncol, 9(3),27. https://doi.org/10.21037/cco.2020.01.06.

Jin, M., Y. Hou, X. Quan, L. Chen, Z. Gao and W. Huang (2021). Smart polymeric nanoparticles with pH-responsive and PEG-detachable properties (II): co-delivery of Paclitaxel and VEGF siRNA for synergistic breast cancer therapy in mice. Int. J. Nanomedicine, 16,5479–5494. https://doi.org/10.2147/IJN.S313339.

Jin, M., B. Zeng, Y. Liu, L. Jin, Y. Hou, C. Liu, W. Liu, H. Wu, L. Chen, Z. Gao and W. Huang. (2022). Co-delivery of repurposing Itraconazole and VEGF siRNA by composite nanoparticulate system for collaborative anti-angiogenesis and anti-tumor efficacy against breast cancer. Pharmaceutics, 14(7), 1369. https://doi.org/10.3390/pharmaceutics14071369.

Jamialahmadi, K., F. Zahedipour and G. Karimi. (2021). The role of microRNAs on doxorubicin drug resistance in breast cancer. J Pharm Pharmacol, 73(8), 997–1006. https://doi.org/10.1093/jpp/rgaa031.

Kopeckova, K., T. Eckschlager, J. Sirc, R. Hobzova, J. Plch, J. Hrabeta and J. Michalek. (2019). Nanodrugs used in cancer therapy. Biomed. Pap. Med. Fac. Univ. Palacky Olomouc Czech Repub., 163(2), 122–131. https://doi.org/10.5507/bp.2019.010.

Korpela, H., O.P. Hätinen, T. Nieminen, R. Mallick, P. Toivanen, J. Airaksinen, K. Valli, M. Hakulinen, P. Poutiainen, J. Nurro and S. Ylä-Herttuala, (2021). Adenoviral VEGF-B186R127S gene transfer induces angiogenesis and improves perfusion in ischemic heart. iScience, 24(12),103533. https://doi.org/10.1016/j.isci.2021.103533.

Karaosmanoglu, S., M. Zhou, B. Shi, X. Zhang, G.R. Williams and X. Chen. (2021). Carrier-free nanodrugs for safe and effective cancer treatment. J. Control Release, 329, 805–832. https://doi.org/10.1016/j.jconrel.2020.10.014

Li, C., H. Wang, H. Fang, C. He, Y. Pei and X. Gai (2021). FOXP3 facilitates the invasion and metastasis of non-small cell lung cancer cells through regulating VEGF, EMT and the Notch1/Hes1 pathway. Exp. Ther. Med., 22(3), 958. https://doi.org/10.3892/etm.2021.10390

Lin, Y.W., S.T. Huang, J.C. Wu, T.H. Chu, S.C. Huang, C.C. Lee and M.H. Tai. (2019). Novel HDGF/HIF-1α/VEGF axis in oral cancer impacts disease prognosis. BMC Cancer, 19(1),1083. https://doi.org/10.1186/s12885-019-6229-5

Luchini, C., L. Pantanowitz, V. Adsay, S.L. Asa, P. Antonini, I. Girolami, N. Veronese, A. Nottegar, S. Cingarlini, L. Landoni, L.A. Brosens, A.V. Verschuur, P. Mattiolo, A. Pea, A. Mafficini, M. Milella, M.K. Niazi, M.N. Gurcan, A. Eccher, I.A. Cree and A. Scarpa (2022). Ki-67 assessment of pancreatic neuroendocrine neoplasms: Systematic review and meta-analysis of manual vs. digital pathology scoring. Mod.

Pathol., 35(6),712–720. https://doi.org/10.1038/s41379-022-01055-1.

LoPresti, S. T., M. L. Arral, N. Chaudhary and K.A. Whitehead (2022). The replacement of helper lipids with charged alternatives in lipid nanoparticles facilitates targeted mRNA delivery to the spleen and lungs. J Control Release, 345, 819 – 831. https://doi.org/10.1016/j.jconrel. 2022.03.046

Mercurio, A.M. (2019). VEGF/Neuropilin Signaling in Cancer Stem Cells. Int. J. Mol. Sci. 20(3):490. https://doi.org/10.3390/ijms20030490.

Maryam, N., S.S. Ahmed, R. Alam, M.U. Hanif, M. Saleem and R. Gul (2021). Role of serum VEGF-A biomarker for early diagnosis of ovarian cancer instead of CA-125. J. Pakistan Med. Assoc., 71(9), 2192–2197. https://doi.org/ 10.47391/JPMA.05-688.

Mainini, F. and M.R. Eccles. (2020). Lipid and polymer-based nanoparticle siRNA delivery systems for cancer therapy. Molecules, 25(11), 2692. https://doi.org/10.3390/molecules25112692.

Mi, X., M. Hu, M. Dong, Z. Yang, X. Zhan, X. Chang, J. Lu and X. Chen (2021). Folic acid decorated zeolitic imidazolate framework (ZIF-8) loaded with Baicalin as a nano-drug delivery system for breast cancer therapy. Int. J. Nanomedicine, 16, 8337–8352. https://doi.org/10.2147/IJN.S340764.

Peng, Y., Y. Wang, N. Tang, D. Sun, Y. Lan, Z. Yu, X. Zhao, L. Feng, B. Zhang, L. Jin, F. Yu, X. Ma and C. Lv (2018). Andrographolide inhibits breast cancer through suppressing COX-2 expression and angiogenesis via inactivation of p300 signaling and VEGF pathway. J. Exp. Clin. Cancer Res., 37(1), 248. https://doi.org/10.1186/s13046-018-0926-9.

Petersen, D.M. S., R.M. Weiss, K.A. Hajj, S.S. Yerneni, N. Chaudhary, A.N. Newby, M.L. Arral and K.A. Whitehead. (2024). Branched-tail lipid nanoparticles for intravenous mRNA delivery to lung immune, endothelial, and alveolar cells in mice. Adv. Healthc Mater, 13(22), e2400225. https://doi.org/10.1002/adhm.202400225

Repp, L., M. Rasoulianboroujeni, H.J. Lee and G.S. Kwon (2021). Acyl and oligo (lactic acid) prodrugs for PEG-b-PLA and PEG-b-PCL nano-assemblies for injection. J. Control Release, 330, 1004–1015. https://doi.org/10.1016/j.jconrel.2020.11.008.

Ramasamy, T., H.B. Ruttala, S. Munusamy, N. Chakraborty and J.O. Kim (2022). Nano drug delivery systems for antisense oligonucleotides (ASO) therapeutics. J. Control Release, 352, 861–878. https://doi.org/10.1016/j.jconrel.2022.10.050.

Swietach, P. (2019). What is pH regulation, and why do cancer cells need it? Cancer Metastasis Rev, 38(1-2), 5–15. https://doi.org/10.1007/s10555-018-09778-x.

Solechan, S., A. Suprihanto, S.A. Widyanto, J. Triyono, D.F. Fitriyana, J.P. Siregar and T. Cionita (2023). Characterization of PLA/PCL/Nano-Hydroxyapatite (nHA) biocomposites prepared via cold isostatic pressing. Polymers (Basel), 15(3), 559. https://doi.org/10.3390/polym15030559.

Vitale, I., G. Manic, L.M. Coussens, G. Kroemer and L. Galluzzi. (2019). Macrophages and metabolism in the tumor microenvironment. Cell Metab., 30(1), 36–50. https://doi.org/10.1016/j.cmet.2019.06.001.

Wang, A. and J.S. Jiang. (2022). Research on mechanism of doxorubicin carried with mesoporous silica nanoparticles mesoporous silica nanoparticles in regulating the activity of liver tumor cells through regulating the activity of Hippo-Yes-Associated protein signal pathway. Sci. Adv. Mater., 14(3), 521–527. https://doi.org/10.1166/sam.2022.4231.

Wu, J. (2021). The Enhanced Permeability and Retention (EPR) effect: the significance of the concept and methods to enhance its application. J. Pers. Med., 11(8), 771. https://doi.org/10.3390/jpm11080771

Zhu, X., L. Chen, B. Huang, Y. Wang, L. Ji, J. Wu, G. Di, G. Liu, K. Yu, Z. Shao and Z. Wang. (2020). The prognostic and predictive potential of Ki-67 in triple-negative breast cancer. Sci. Rep., 10(1), 225. https://doi.org/10.1038/s41598-019-57094-3.

Zhang, X., Z. Wu, Y. Peng, D. Li, Y. Jiang, F. Pan, Y. Li, Y. Lai, Z. Cui and K. Zhang. (2021). Correlationship between Ki67, VEGF, and p53 and hepatocellular carcinoma recurrence in liver transplant patients. Biomed. Res. Int., 2021, 6651397. https://doi.org/10.1155/2021/6651397.